

Design, Fabrication and Testing Of Flapping Wing Micro Air Vehicle

K. P. Preethi Manohari Sai¹, K. Bharadwaj², K. Ravi Teja³, Kalyan Dagamoori⁴, Kasiraju Venkata Sai Tarun⁵, Vishnu Vijayan⁶

^{1,2,3,6}B.Tech Student, Department Of Aeronautical Engineering, MLR Institute Of Technology, Dundigal, Hyderabad. INDIA.

⁴B.Tech Student, Department Of Aeronautical Engineering, MLR Institute Of Technology and Management, Dundigal, Hyderabad. INDIA.

⁵B.Tech Student, Department Of Aeronautical Engineering, GITAM UNIVERSITY, Hyderabad. INDIA.

ABSTRACT:

Flapping flight has the potential to revolutionize micro air vehicles (MAVs) due to increased aerodynamic performance, improved maneuverability and hover capabilities. The purpose of this project is to design and fabrication of flapping wing micro air vehicle. The designed MAV will have a wing span of 40cm. The drive mechanism will be a gear mechanism to drive the flapping wing MAV, along with one actuator. Initially, a preliminary design of flapping wing MAV is drawn and necessary calculation for the lift calculation has been done. Later a CAD model is drawn in CATIA V5 software. Finally we tested by Flying.

Keywords : Flapping wing mav, Ornithopter, Components of MEMS etc.

I. INTRODUCTION :

An ornithopter(from Greek ornithos "bird" and pteron "wing") is an aircraft that flies by flapping its wings. Designers tend to imitated by the flapping-wing flight of birds, bats, and insects. Through machines may differ in form, they are usually built on the same scale as these flying creatures. Manned ornithopter have also been, and some have successful. An ornithopter is an aircraft that flies by flapping its wings. Inspired by nature, we intend to design our own ornithopters by studying the kinematics and dynamics of flapping wing. Also, to fabricate the remote controlled flapping wing MAV. A gear box is needed to be constructed to bring down the rpm to a reasonable value so that the wing flapping frequency becomes 2-4 Hz. Next we need harness the vertical velocity of the rotating gear using the simple concept of simple harmonic motion. In aircraft, tail is used for the pitch and yaw motion whereas in ornithopter tail is used for pitch motion. The ornithopter can be used for various kind of spying and surveillance by fabricating better construction material and gears. Ornithopter can be used for military application, such as aerial reconnaissance without alerting the enemies that they are under surveillance as they can be resembled into birds or insects.

1.1 History

The ancient Greek legend of Daedalus (Greek demigod engineer) and Icarus (Daedalus's son) and The Chinese Book of Han(19 AD) both describe the use of feathers to make wings for a person but these

are not actually aircraft. Some early manned flight attempts may have been intended to achieve flapping-wing flight though probably only a glide was actually achieved. , Leonardo da Vinci began to study the flight of birds.

He grasped that humans are too heavy, and not strong enough, to fly using wings simply attached to the arms. Therefore he sketched a device in which the aviator lies down on a plank and works two large, membranous wings using hand levers, foot pedals, and a system of pulleys.

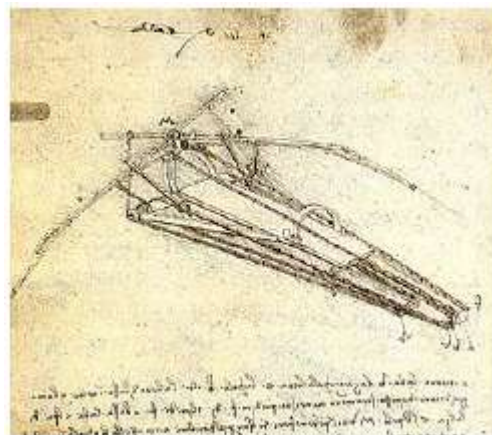


Fig 1.1.1 Leonardo da Vinci's Ornithopter Design

The first ornithopters capable of flight were constructed in France. Jobert in 1871 used a rubber band to power a small model bird. Alphonse

Penaud, Abel Hureau de Villeneuve, and Victor Tatin, also made rubber-powered ornithopters during the 1870s. Tatin's ornithopter was perhaps the first to use active torsion of the wings, and apparently it served as the basis for a commercial toy offered by Pichancourt c. 1889. Gustave Trouve was the first to use internal combustion and his 1890 model flew a distance of 70 metres in a demonstration for the French Academy of Sciences. The wings were flapped by gunpower charges activating a bourbon tube.

1.2 Manned Flight

Manned ornithopters fall into two general categories: Those powered by the muscular effort of the pilot (human-powered ornithopters), and those powered by an engine.

Otto Lilienthal in 1894, an aviation pioneer became famous in Germany for his widely publicized and successful glider flights. Lilienthal also studied bird flight and conducted some related experiments. He constructed an ornithopter, although its complete development was prevented by his untimely death on the 9th of August 1896 in a glider accident.



Fig. 1.2.1 Otta Lilienthal on August 16, 1894 with his kleinerSchlagflügelapparat

AlexandraLippisch in 1929, a man-powered ornithopter designed by him (designer of the Me163 Komet) flew a distance of 250 to 300 metres after tow launch. Since a tow launch was used, some have questioned whether the aircraft was capable of flying on its own. Lippisch asserted that the aircraft was actually flying, not making an extended glide. (Precise measurement of altitude and velocity over time would be necessary to resolve this question.) Most of the subsequent human-powered ornithopters likewise used a tow launch, and flights were brief simply because human muscle power diminishes rapidly over time.

Adalbert Schmid in 1942, made a much longer flight of a human-powered ornithopter at Munich-Laim. It travelled a distance of 900 metres, maintaining a height of 20 metres throughout most of the flight. Later this same aircraft was fitted with a 3 hp (2.2 kW) Sachs motorcycle engine. With the engine, it made flights up to 15 minutes in duration. Schmid later constructed a 10 hp (7.5 kW)

ornithopter based on the Grunau-Baby Ila sailplane, which was flown in 1947. The second aircraft had flapping outer wing panels.

A team at the University of Toronto Institute for Aerospace Studies, headed by Professor James DeLaurier, worked for several years on an engine-powered, piloted ornithopter. In July 2006, at the Bombardier Airfield at Downview Park in Tronto, Professor DeLaurier's machine, the UTIASOrnithopter No. 1 made a jet-assisted takeoff and 14-second flight. According to DeLaurier, the jet was necessary for sustained flight, but the flapping wings did most of the work.

Todd Reichert of the University of Toronto Institute for Aerospace Studies, on August 2, 2010 has piloted a human-powered ornithopter named Snowbird.

The 32-metre (105 ft 0 in) wingspan, 42-kilogram (93 lb) aircraft was constructed from carbon fiber, balsa, and foam. The pilot sat in a small cockpit suspended below the wings and pumped a bar with his feet to operate a system of wires that flapped the wings up and down. Towed by a car until airborne, it then sustained flight for almost 20 seconds. It flew 145 metres with an average speed of 25.6 km/h (7.1 m/s). Similar tow-launched flights were made in the past, but improved data collection verified that the ornithopter was capable of self-powered flight once aloft.

1.3 Applications for unmanned ornithopters

Practical applications capitalize on the resemblance to birds or insects. He Colorado Division of Wildlife has used these machines to help save the endangered Gunnison Sage Grouse. An artificial hawk under the control of an operator causes the grouse to remain on the ground so they can be captured for study.

AeroVironment, Inc., then led by Paul B MacCready (Gossamer Albatross) developed in the mid-1980s, for the Smithsonian Institution, a half-scale radio-controlled replica of the giant pterosaur, Quetzalcoatlusnorthropi. It was built to star in the IMAX movie On the Wing. The model had a wingspan of 5.5 metres (18 feet) and featured a complex computerized autopilot control system, just as the full-size pterosaur relied on its neuromuscular system to make constant adjustments in flight.

Researchers hope to eliminate the motors and gears of current designs by more closely imitating animal flight muscles. Georgia Tech Research Institute's Robert C. Michelson is developing a Reciprocating Chemical Muscle for use in micro-scale flapping-wing aircraft. Michelson uses the term "entomopter" for this type of ornithopter. SRI International is developing polymerartificial muscles which may also be used for flapping-wing flight.

1.4 Successful flapping wing MAVs

Percival Spencer constructed a series of engine-driven ornithopters in the shape of a bird. They ranged in size from a small 0.02-engine-powered ornithopter to one with an eight-foot wingspan. Spencer is also noted as a pioneer pilot and the designer of the Republic Seabee amphibious airplane. He also designed a toy, called the Wham-O Bird, which introduced thousands of children to the idea of mechanized flapping-wing flight.



Fig. 1.4.1 Wham-O Bird

Sean Kinkade's Skybird, based somewhat on the Spencer Seagulls and using a 0.15 methanol-fueled engine, was an attempt at small-scale commercial production of an RC ornithopter. Smaller, electric versions were later offered. Unfortunately, many would-be enthusiasts paid their money and never received the product.



Fig. 1.4.2 Skybird

Several successful fabrication of flying birds including hovering bird with wing span of 30cm to 100cm. The project, aims at taking this research forward by building an autonomous, 1.5m wing span flying bird which will carry a small camera as payload and will be able to take pictures for surveillance.



Fig. 1.4.3 IIT Kanpur developed flapping wing MAV

Robert Masters began a series of RC ornithopters with foam, actively twisted wings. The appearance of these ornithopters is close to that of a real bird and they are being offered for use in bird control at airports.



Fig. 1.4.4 Robert Master's Ornithopter

II. LITERATURE SURVEY :

Alphonse Penaud, in 1870's performed a mechanical flapping wing rubber powered model ornithopter in France, which was documented and witnessed. Alexander Lippisch also worked on ornithopters[1]. During 1990's The Project Ornithopter engine powered piloted aircraft was which is based on the technology of the Harris/DeLaurier model. One of the first successful attempts to develop bird-like flapping flight was by DeLaurier[2].

The first MAVs were developed as early as WW-I in the form of guided munitions later expanding their roles into radio controlled target drones, reconnaissance aircraft and glide bombs of the modern day cruise missile[3]. The first radio controlled(RC) aircraft flight in Germany 1936 led the way to further refinement of small UAVs in post war era. The air flow field in flapping wings can not be assumed as steady. A large angle of attack would lead to flow separation and turbulences too. Obviously, there must be phenomena producing

extra lift. As was discovered with the development of MEMS technology, the physics of the small are different from that of the large (for example, friction is more important than gravity) [4]. For MEMS technology to progress, researchers had to develop a new understanding of these physics, and develop new techniques for overcoming and capitalizing on them. This is the case with small scale, or low Re aerodynamics today.

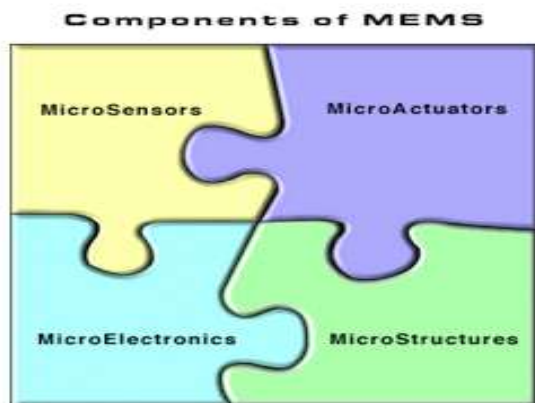


Fig. 2 Components of MEMS

2.1 Mechanics of Bird

Bird flight is one of the natural example of flapping flight. For the birds, the feather on their wings are instrumental in their achieving flight, both the prouisionand the efficient aerodynamics[5]. There are two sets of feathers on a bird's wing, namely the primary and secondary feathers. The primary feathers are attached to the hard bones, and are found on the hand section. Flight will be impossible without the primary feathers. The secondary feathers, which are inserted along the arm, which is the inner wing, are responsible for lift. The bird is able to enjoy much freedom of movement during flight because of the wing's ability to have its shape altered, which is the result of each feather functioning independently.

During flapping flight, the inner wing gives lift whilst the hand section provides thrust [6] The inner part of a bird's wing remains relatively stationary and acts as an aerofoil, producing lift and drag [7]. On the backstroke, which is the power stroke, the primary feathers are linked together to produce a near perfect aerofoil. Since the outer part of the wing is more mobile, it can be twisted so that the wing points into the airstream; as with all aerofoils, forces are generated and maximum thrust and minimum drag is obtained in addition to lift. On the upstroke, the primary concern is to reduce drag. This is achieved through different mechanisms for different species of birds. On the smaller birds, the primary feathers are separated, allowing air to pass through and thus considerably reducing drag [6]. For the

larger birds or small but long-winged birds, their wings are typically either flexed or partially closed on the upstroke.

2.2 Experimental Studies

Wing Frequencies were observed in the field for 32 morphologically diverse bird species, representing 18 families and ranging in mass from 20g to nearly 5kg. A combination of multiple regression and dimensional analysis was used to show that wing frequency(f) may be estimated by:

$$f = 1.08 (m^{1/3} g^{1/2} b^{-1} S^{-1/4} \rho^{-1/3})$$

where m is the bird's body mass, g is the acceleration due to gravity, b is the wing span, S is the wing area and ρ is the air density[8].

An experimental study was conducted to assess the aerodynamic benefits of flapping compared with fixed soaring flight for the development of flapping wing Micro Air Vehicle(MAVs). The time averaged aerodynamic performance(i.e. a flexible nylon wing and a very flexible latex wing) were compared with that of a conventional rigid wing to evaluate the effects of skin flexibility of the tested wing son their aerodynamic performance for flapping flight application[9].

In the present, an experimental investigation was 7 conducted to assess the aerodynamics benefits of using flexible membrane airfoil/wings for flapping wing MAV applications. The time averaged lift and thrust generated by flapping two flexible with different skin flexibility were compared with those of a conventional rigid wing to quantify the effects of the skin flexibility of the tested wings on their aerodynamic performances[9].

2.3 Computational Studies

Micro Air Vehicles (MAVs) by virtue of their small size and maneuverability can provide an indispensable vehicle for advance surveillance and reconnaissance missions. MAVs by equirement are compact with dimensions less than 15-20 cm and flight speeds of around 10-15 m/s with gross takeoff weights of 200g or less and which operate in the low Reynolds number (10,000-100,000) regime. At these low Reynolds numbers, the aerodynamic efficiency (lift to drag ratio) of conventional fixed airfoils rapidly deteriorates due to boundary layer separation and early onset of stall[10].

Vortex wake effects were also accounted for in the model that DeLaurier (1993a) developed. His computational model for the unsteady aerodynamics of root-flapping wing was based on the modified

strip theory approach, which made use of the concept of dividing the wing into a number of thin strips. This enabled the study of the wing as a set of aerofoils next to one another by assuming no crossflow between the strips or sections. Vortex-wake effects were accounted for using modified Theodorsen functions. In addition, this model differed from previous work in that camber and leading edge suction effects, as well as post stall behaviour, were also accounted for. The analysis was based on the assumptions that the flapping wing is spanwise rigid, has high wing aspect ratio such that the flow over each section is essentially chordwise, and that the wing motion is continuous sinusoidal with equal times between upstroke and downstroke. The model allowed the calculation of average lift, thrust, power required and propulsive efficiency of a flapping wing in equilibrium flight. A numerical example was demonstrated to predict the performance of a mechanical flying Pterosaur replica, constructed by AeroVironment (1985), and the results were presented.

Shyyet al. (2000) studied and reviewed the computational model proposed by DeLaurier (1993a). They performed computations for the mechanical flying Pterosaur replica using a Matlab-code developed based on the model and the results are compared with those presented by DeLaurier. They further investigated the performance of smaller biological bird species, with results presented. They also studied the effects of aerodynamic parameters such as the flapping axis angle, maximum flapping angle amplitude and dynamic twist of the wing, on the performance of the biological flapping flight. In addition, the authors developed an optimization procedure for obtaining maximum propulsive efficiency within the range of possible flying conditions. However, flexing of the biological wings, which tend to produce useful aerodynamic benefits, have yet been incorporated since the model used assumes that the wing is spanwise rigid.

KINEMATICS OF FLAPPING WING :

Human has a desire to fly like the flying biosystems such as the insects and bird through engineering to meet the motivational creativity and a hundreds of years dream shown in Leonardo Da Vinci's drawing of Otto Lilitenthal's gliders, to modern aircraft and present flapping wing research.

3.1 Aerodynamics of Flapping Wing

Flapping aerodynamics is studied as an unsteady aerodynamic flow. As for larger bird, the flapping rate is low whereas for smaller bird and insects rate is more due to highly unsteady aerodynamics and lesser trailing vortices. Small birds and insects has to work harder to producer the trailing vortices, to

increase the viscous flow regime. To enhance the lift bird and insects has several other mechanisms are been used such as Clap and Fling Mechanism Wake Capture, Rapid Pitch Up and Delayed Stall[12].

Kinematics of Wing

The flapping wing motion ornithopters and entomopters can have three basic motion with respect to axis based on the kinematics motion of wing and mechanism of force generation a) Flapping , which is up and down plunging motion of the wing . Flapping produces the majority of the bird's or insect's power and has the largest degree of freedom. b) Feathering is the pitching motion of wing and can vary along the span. c) Lead-Lag, which is in-plane lateral movement of wing[12].

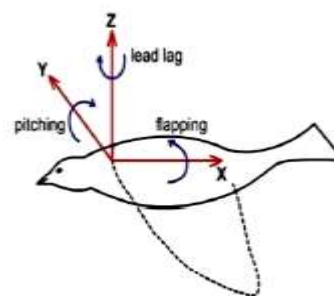


Fig. 3.1.1 Moments on Wing

Flapping Wing Forces

Flapping motion involves two stage: the Down Stoke, which provide the majority of the thrust and the Up stoke which can also (depending on the birds wing) provide some thrust. At some thrust at each up-stroke the wing is slightly folded inwards to reduce the energetic cost of flapping with flight . Birds change the angle between the up stroke and the down stroke of their wing. During the down stroke of their wing. During the down stroke the angle of attack is increased and is decreased during the up stroke.

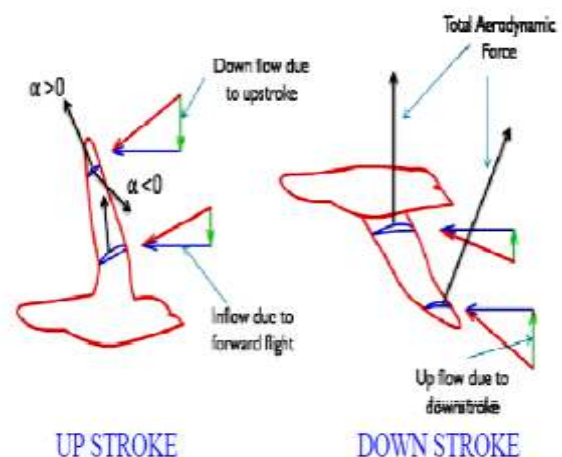


Fig 3.1.2. Forces acting on Flapping Wing

During the down stroke the total aerodynamic force is tilted forward and has two components, lift and thrust. During up stroke, the AOA is always positive near the root but at the tip it can be positive or negative depending on the amount of pitching up of wing. Therefore, during up stroke the inner part of wing produces aerodynamic force which is upward but tilted backwards producing lift and negative thrust. The outer region of the wings would produce positive lift and drag if the AOA is positive. But if AOA is negative then it will produce negative lift but positive thrust [12]. Both cases are depicted in the fig. 3.1.2.

3.2 Flapping Frequency

In the present research, Pennycuick has made some observations in the flapping frequency which has been considered. Pennycuick found out multiple regression and dimensional analysis by conducting an experimental studies on 32 morphologically diverse bird species, representing 18 families, and ranging mass from 20g to 5kg. The wingbeat frequency is correlated by the following formula

$$f = 1.08 (m^{1/3} g^{1/2} b^{-1} S^{-1/4} \rho^{-1/3})$$

where m is the bird's body mass, g is the acceleration due to gravity, b is the wing span, S is the wing area and ρ is the air density[8].

The relationship between flight speed & the mass of the bird can be given by from Pennycuick,

where m is the mass of the bird and U is the flight speed.

$$U = 4.77 m^{\frac{1}{6}}$$

From Greenwalt computed statistical data,

$$f l^{1.16} = 3.54$$

where, f is flapping frequency and l wing length(cm)

While Azuma showed the relation,

$$f (\text{large birds}) = 116.3 m^{-\frac{1}{6}}$$

$$f (\text{small birds}) = 28.7 m^{-\frac{1}{3}}$$

where f is flapping frequency and m is mass of bird.

3.3 Aerodynamics Calculations

This procedure basically follows pitching-flapping motion of rigid wing that is a structured adaptation and simplification of the procedure adopted by DeLaurier, Harmon, Malik et al. and Zakaria et al.

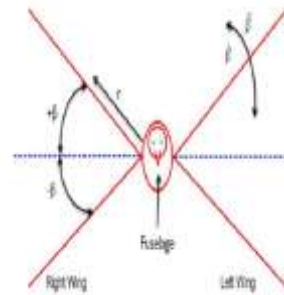


Fig 3.3.1. Front View of Flapping Wing

Flapping angle varies β as sinusoidal function. β and its rate are given by following equations. The degree of freedom of the motion is depicted in Fig. 3. Flapping angle β varies as sinusoidal function. The β angle and its rate and pitching angle θ are given by

$$\beta(t) = \beta_{\max} \cos 2\pi f t$$

$$\dot{\beta}(t) = -2\pi f t \sin 2\pi f t$$

$$\theta(t) = \frac{r(i)}{B} \theta_0 \cos(2\pi f t + \phi)$$

where, θ_0 is the pitching motion, $\beta(t)$ is the

flapping angle and $\dot{\beta}(t)$ is the flapping rate.

The horizontal and vertical components of relative wind velocity as under:-

$$V_x = U \cos(\delta) + (0.75.c.\dot{\theta}.\sin(\theta))$$

$$V_y = \sin(\delta) + (-r(i).\dot{\beta}.\cos(\beta)) + (0.75.c.\dot{\theta}.\cos(\beta))$$

for horizontal flight, the flight path angle γ is zero.

Also $0.75.c.\dot{\theta}$ is the relative air effect of the

pitching rate $\dot{\theta}$ which is manifested at 75% of the chord length[13].

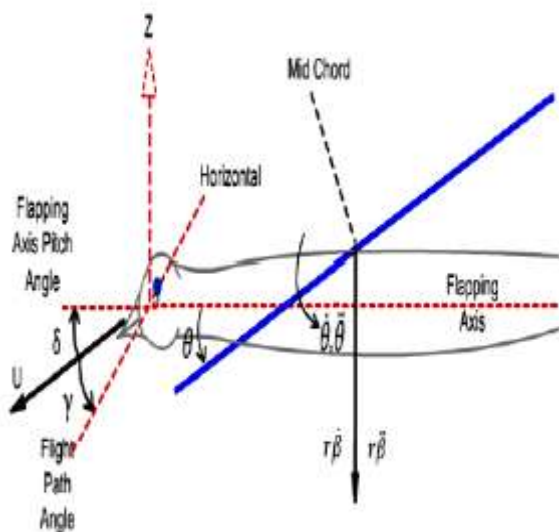


Fig.3.3.2 Side View of Flapping Motion

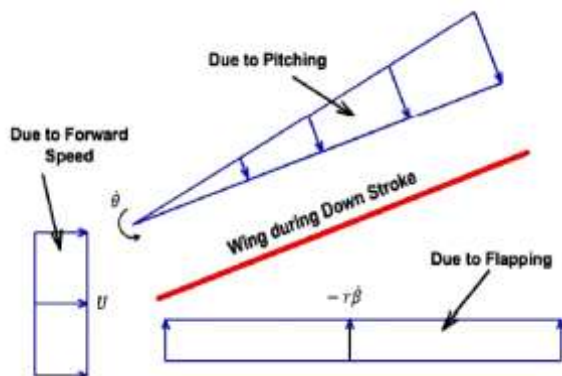


Fig. 3.3.3 Relative Flow of Air [12]

Now we can find out relative velocity, relative angle between the two velocity components ψ and the effective AOA as under:-

$$V_{rel} = \sqrt{V_x^2 + V_y^2}, \psi = \tan^{-1} \left(\frac{V_x}{V_y} \right),$$

$$\alpha_{eff} = \psi + \theta$$

The section lift coefficient due to circulation (Kutta-Joukowski condition, flat plate) is given by

$$C_{l-c} = 2\Pi C(k) \sin \alpha_{eff}$$

The section lift can thus be calculated by:-

$$dL_c = \frac{1}{2} \rho V_{rel}^2 C_{l-c} \cdot c \cdot dr$$

which is to be integrated for entire wingspan. where c and dr are the chord length and width of the element of wing under consideration. The apparent mass effect (momentum transferred by accelerating air to the wing) for the section, is perpendicular to

the wing, and acts at mid chord, and can be calculated as

The drag force has two components, profile drag dD_p and induced drag dD_i . These are calculated as under:-

$$dD_p = \frac{1}{2} \rho V_{rel}^2 C_{dp} \cdot c \cdot dr$$

$$dD_i = \frac{1}{2} \rho V_{rel}^2 C_{di} \cdot c \cdot dr$$

Total section drag is thus given by:-

$$dD_d = dD_p + dD_i$$

Now, we have resolve horizontal and vertical component of the forces given by:-

$$dF_{ver} = dL_c \cos \psi \cdot \cos \delta + dN_{nc} \cos(-\theta) \cdot \cos \beta \cdot \cos \delta$$

$$dF_{hor} = dL_c \sin \psi \cdot \cos \delta + dN_{nc} \sin(-\theta) \cdot \cos \delta - dD_d \cos \psi \cdot \cos \delta$$

adding all the vertical and horizontal components of forces will give the lift and thrust of the ornithopter for that instance of time for which the calculations

$$dN_{nc} = -\frac{\rho \Pi c^2}{4} (\dot{\theta} U + r \ddot{\beta} \cos \theta - 0.5 \ddot{\theta}) dr$$

are being done.

3.4 Flapping Wing in a Spring Mass System

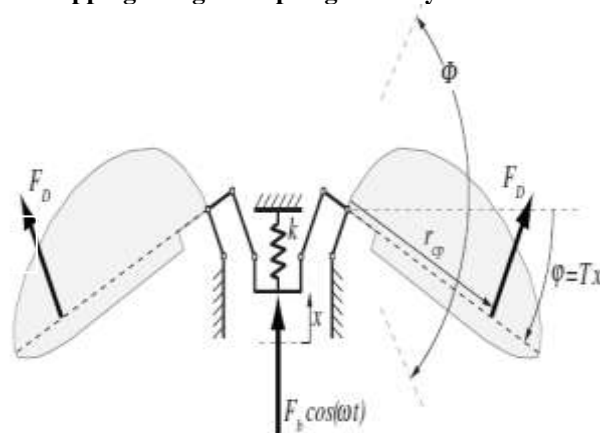


Fig. 3.4.1 Canonical flapping configuration consistent with our model; a single linear actuator drives both wings symmetrically through an (assumed) linear transmission, as viewed normal to the stroke plane.

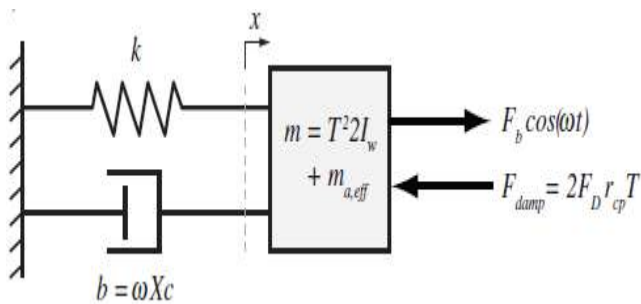


Fig. 3.4.2 Equivalent LP linear model used in our analysis.

The system of the actuator and transmission wing system of a flapping vehicle is an equivalent to one degree of freedom (DOF) lumped parameters (LP) linear model, characterized by effective mass, stiffness and damping coefficients. Fig. 3.4.1 shows a simplified flapping configuration with a single power actuator driving two wings, and the equivalent translational LP model. We assume that the wings flap symmetrically in a horizontal stroke plane, with peak-to-peak flapping amplitude ϕ . The wings are coupled to the drive actuator through a linear, lossless transmission with transmission ratio T , where the time-varying flapping angle $\phi(t)$ and actuator displacement $x(t)$ are related by $\phi = Tx$. [13].

PROTOTYPE DESIGN AND FABRICATION :

The focus is shifted to design the MAV as gone through the literature to enhance the knowledge of the motion of flapping wings and how they generate lift. Previous projects involving flapping wing MAVs has provided a foundation from which MAV can be design.

The process of design and modelling begins with a basic idea of fabricating a flapping wing vehicle capable of takeoff and landing, hover and horizontal flight to achieve with this project. While literature survey it has been decided that to mimick a bird would be difficult and unreasonable, for these animals move in a very complex manner. Through more research it is found out that elliptical shape wing are designed more in previous flapping wing MAVs due to its simpler aerodynamic shape and theoretical calculations.

4.1 Basic Flapping Wing Theory

Flapping flight is more complicated than flight with fixed wings but still the basic concept of aerodynamics of fixed wing can be applied. The thin membrane of flexible material can be stucked on the leading edge and root chord of the wing. The thin membrane are used for the wing is non-woven fibre and cellos plastic.

According to the Ornithopter Design Manual (Chronister, 1996) and Micah O'Halloran (1998), membrane wings generate positive lift and thrust during the downstroke. However, during upstroke, the lift becomes negative although thrust is still positive. The material of the membrane is flexible. Hence during downstroke, as shown in Fig. 4.1, air is displaced downward and backward, causing the membrane to be pushed upward and forward. The direction of this force will produce lift and thrust. Although the front of the membrane is glued to the leading edge, the trailing end is allowed to swivel within the limits of the flexible material. This will cause the trailing edge to always lag behind the leading edge. As a result, the membrane will become positively cambered.

From fixed wing aerodynamics, the camber shape will provide some additional lift as well.

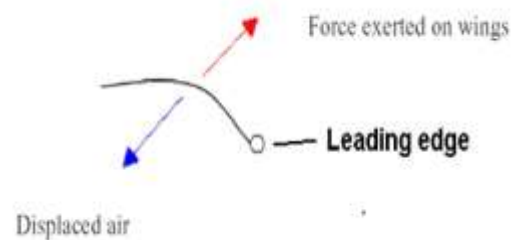


Fig. 4.1.1 Wing Membrane Downstroke

During the upstroke, as shown in Fig. 4.2, the reverse happens and the trailing edge is always lower than the leading edge. The new direction of force will provide thrust but negative lift.

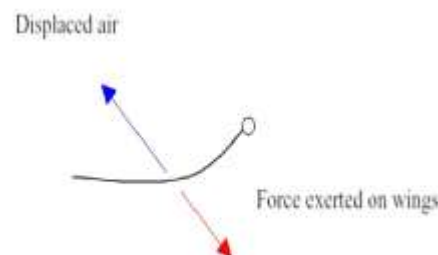


Fig. 4.1.2 Wing Membrane Upstroke

Throughout the whole flapping cycle, the net force will only be the thrust because the positive and negative lift cancel each other out. In order to obtain lift, the forces must be redirected by increasing the pitch of the wing. In ornithopter's design, this is usually achieved using the tail. The tail is tilted slightly upwards and this will cause the wing to pitch up during flight (Fig. 4.1.3).

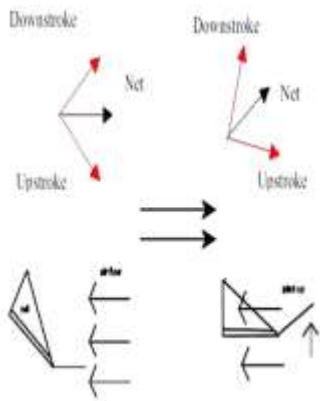


Fig. 4.1.3 Pitching of ornithopter to achieve net lift

4.2 Wing Design

One of important process of this project is wing design and its development. The wing has semi-span of 20cm having an half elliptical shape. The wing has root chord of 18cm. The wing has an area of 565 sq.cm. The aspect ratio of wing is 2.22. The leading edge and root of wing structure is been fabricated by using balsa wood of 3mm thickness. Non-woven fabric is using for wing membrane.



Fig. 4.2.3 Wing Layout

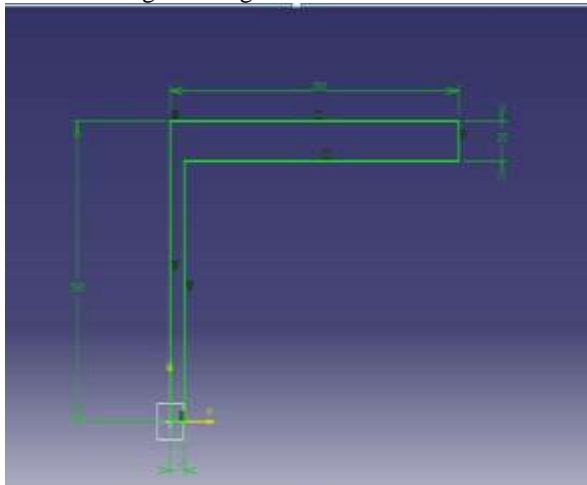


Fig. 4.2.1: Dimensions of Wing

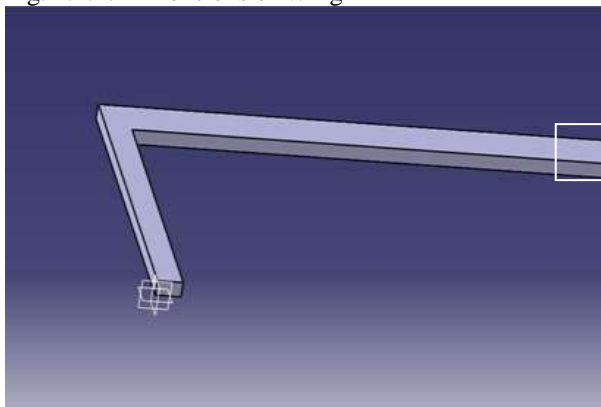


Fig. 4.2.2: Wing Geometry

4.3 AIRFRAME

Airframe of the MAV has a length of 38cm. It is made by fiber plastic. On the airframe, the gear mechanism is mounted.

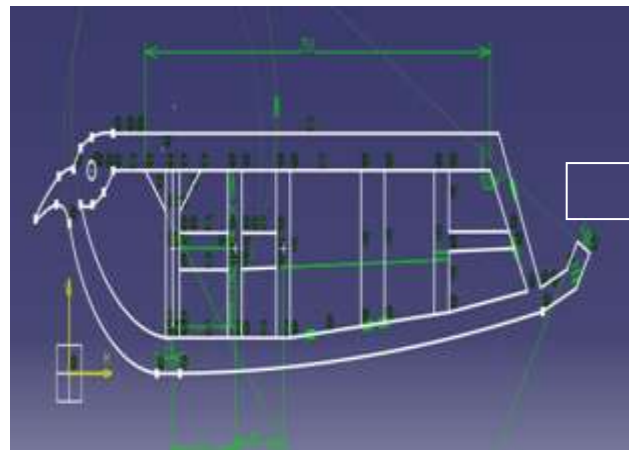


Fig. 4.3.1 Airframe Dimension

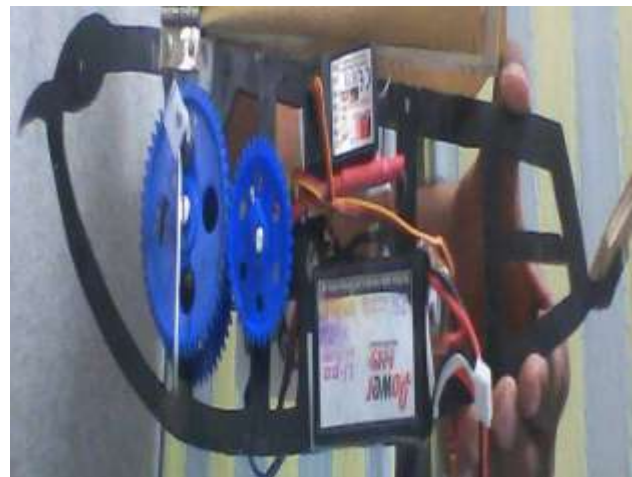


Fig 4.3.2 Airframe Structure

4.4 Flapping Mechanism

The main objective of flapping mechanism is to convert the motor's rotary motion into flapping motion. It is the most important component of the MAV thus much research was done to assess the many different designs available. Generally the mechanism design is about the same to each other with only slight modifications.

Types of Mechanism

Staggered Crank Design

The staggered crank design in Fig. 4.4.1 is the most basic of the flapping wing design. The connector rods are staggered in a measured distance and angle to ensure that the left and right wing are flapping symmetrically. This design is favoured by hobbyist who wants to attempt to make their own Ornithopter using household items. Modifications has to be made so that the motor can be used instead of a rubber band as its power source.

Single Gear Crank

The single gear crank design in Fig. 4.4.2 taken from University of California Biomimetic Millisystems Lab, looks simple however it is more complicated than it seems. Fig. 4.4.2 shows the wings at the same level. The centre point where the connector rod and the wing hinges are connected to each other has to expand and contract as the mechanism flaps. Contracting and expanding at a very high frequency could result in component failure.



Fig. 4.4.2 Single Gear Crank

Dual Gear Crank Design

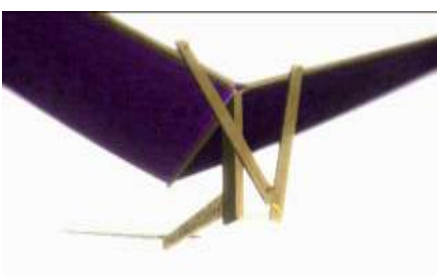


Fig. 4.4.3, taken from a published paper, shows the dual gear crank design from similarly used in the Festo's SmartBird [10]. It features 2 gears that controls each wing hinges separately. There are different variation to the drivetrain design. The one shown in Fig.4.4.3, uses the pinion wheel to drive both the secondary gears. The secondary gears will rotate in the same direction with each other. The other design, has the pinion gear rotate the secondary gear and this secondary gear to another secondary gear. The secondary gears would rotate counter clockwise to each other. This design is much simpler to implement and reduce the wing symmetry misalignment.

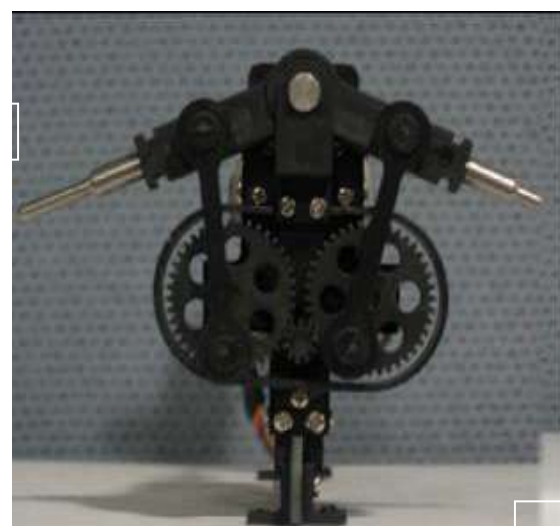


Fig. 4.4.3 Dual Gear Crank

Equation of Motion for Mechanism

Muller, gave few mechanism along with the equation of the motion of the each of the mechanism:

a) Direct Mechanism

Fig. 4.4.4 shows the direct mechanism in which the wing is directly attached the motor. In this mechanism, alternating the input signal does the flapping of wing . The frequency and amplitude the input signal does the flapping of the wings. The flapping and amplitude are not predefined and can be adjusted in this type of mechanism.



Fig.4.4.4 Direct Actuation

The equation of the motion is given as:

$$\theta_w \ddot{\varphi} = M_m - F_d \cdot l$$

where, θ_w is the moment of inertia of the wing

M_m is motor torque

F_d is aerodynamic drag force and

l is the characteristic length of the wing

b) Actuation with Mechanism

The mechanism is consists of four-bar linkage. The amplitude is adjusted with length of the links and is predefined as shown in Fig. 4.4.5. This design doesn't need an alternating input signal.

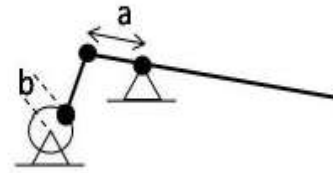


Fig. 4.4.5: Actuation with Mechanism

The equation of the motor angle is:

$$\theta_m \ddot{\alpha} = M_m - b \cos(\alpha) \cdot F$$

Where F is the force in the joint c

The equation of motion for the wing angle is:

$$\theta_w \ddot{\varphi} = F_d \cdot l - a \cos(\varphi) \cdot F$$

The equation of motion for the four - bar mechanism is given therefore as:

$$\ddot{\alpha} = \frac{1}{\theta_m + \frac{c \cos(\alpha) \theta_w \varphi_o \cos(\alpha)}{a \cos(\varphi_o \sin \alpha)}} \cdot \left(M_m - \left(\frac{b \cos \alpha}{a \cos(\varphi_o \sin \alpha)} \right) \cdot [F_d \cdot l - \theta_w \varphi_o \sin(\alpha) \dot{\alpha}^2] \right)$$

c) Mechanism combined with torsional spring

This mechanism is same as mechanism in shown in section b with a minor difference that there is a torsional spring in the wing shown in Fig. 4.4.6. The advantage of this system is that the amplitude of the wing is amplified much more than the amplitude of the bar-mechanism.

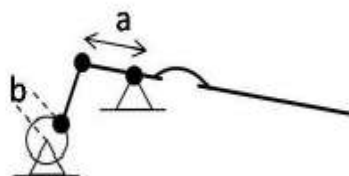


Fig. 4.4.6 Combined With Torsional Spring

The equation of the motion for the wing angle is given as follows:

$$\theta_w \ddot{\varphi} = k(\beta - \varphi) + F_d \cdot l$$

The equation of motion for four-bar linkage is given as:

$$\theta_m \ddot{\alpha} = M_m - \left(\frac{b \cos \alpha}{a \cos(-\beta \sin \alpha)} \right) \cdot (k(\beta_o \sin \alpha + \varphi))$$

MAV's Gear Mechanism

Gear mechanism for MAV considered is dual crank mechanism which slightly modified due to place constraint in the airframe.



(a)



(b)



(c)

Fig.4.4.7 Gear Mechanism of MAV

In this mechanism the driving gear is attached to the motor having a maximum speed of 6000rpm and runs at the 1326kv. Then the driven gear is connected to the one driven gear which mounted on the 6mm diameter shaft along with it another gear is mounted on shaft. Both the gear are installed with a cranking shaft at a offset distance of 25mm from center. On the crank shafts two control rods of length 50mm are linked. The control rod length is determine by practically by figuring out length covered by the cranks from bottom to top or vice verse. As the cranks are placed at the distance 25mm from center then from top to bottom stroke length will be 50mm.

RESULTS :

APPENDICES A: LIFT CALCULATIONS

Table A:1 shows the notation in the Table A:2.

B	Semi span
β_{max}	Maximum flapping angle
θ	Pitching angle
r(i)	Distance along the span of the wing element i
V_x	Horizontal velocity
V_y	Vertical velocity
V_{rel}	Relative velocity
ψ	Relative angle
α_{eff}	Effective AOA
C_{l-c}	Lift coefficient due to circulation
C(k)	Theodorsen Lift Deficiency
k	Reducing frequency
C_1 and C_2	Constant
AR	Aspect Ratio
dr	Width of element
dL _c	Lift in element of width dr
Re ref.	Reference Reynolds number
e	Efficiency factor
C_f	Skin friction coefficient
C_{Dp}	Drag coefficient
C_{di}	Induced drag coefficient
dN _{nc}	Normal force
dF _{ver}	Vertical components of force

Table A:2 below shows the data to calculate the lift distribution of flapping wing along the wing span of 40cm.

Flapping Rate Calculation			Pitching Angle Calculation		
β_{max}	30		B	27	
t	2		$\dot{\theta}$	4	
θ	12.5714286				
Freq.	$\beta(t)$	$\dot{\beta}(t)$	r(i)	$\theta(t)$	$\dot{\theta}(t)$
3	29.9982217	-0.2053155	0	0	0
3.05	24.0738299	-11.439679	2	-0.35721	-6.90139
3.1	8.94891702	-18.598589	4	-0.78956	5.01887
3.15	-9.5960873	-18.759739	6	-0.84444	33.75888
3.2	-24.473665	-11.633095	8	-0.24242	63.61543
3.25	-29.997913	0.2409597	10	0.917175	72.60709
3.3	-24.057577	12.392456	12	2.144212	44.72177
3.35	-8.9229322	20.104166	14	2.763063	-19.0882
3.4	9.62187367	20.242397	16	2.249784	-97.2557
3.45	24.4893979	12.525873	18	0.542205	-154.339
3.5	29.9975796	-0.2794552	20	-1.83757	-156.311
3.55	24.0413052	-13.347509	22	-3.93285	-88.0421
3.6	8.89694005	-21.610575	24	-4.73597	35.35916
3.65	-9.6476521	-21.724122	26	-3.65254	169.8133
3.7	-24.505111	-13.416313	28	-0.83841	257.5149
3.75	-29.997221	0.3208019	30	2.761195	251.0965
3.8	-24.025013	14.304836	32	5.723105	136.8316
3.85	-8.8709406	23.117812	34	6.708288	-53.8654
3.9	9.67342253	23.204913	36	5.052714	-251.455
3.95	24.5208031	14.304413	38	1.131019	-373.149
4	29.9968387	-0.3649997	40	-3.68804	-356.947
4.05	24.0087014	-15.264436	42	-7.51498	-191.06
4.1	8.84493378	-24.625872	44	-8.68	74.64053
4.15	-9.699185	-24.684766	46	-6.4503	342.206
4.2	-24.536475	-15.190171	48	-1.42004	501.2469
4.25	-29.996431	0.4120486	50	4.618096	473.8464
4.3	-23.99237	16.226305	52	9.308478	250.6955
4.35	-8.8189197	26.134754	54	10.65111	-97.7184
4.4	9.72493953	26.163676	56	7.845284	-442.089
4.45	24.5521275	16.073583	58	1.705473	-641.812
4.5	29.995999	-0.4619484	60	-5.55137	-601.779

Aerodynamics Calculation				
		U(m/s)	4	
		δ	6	
		c	13	
V_{x1}	V_{y1}	V_{rel}	ψ	α_{eff}
3.840681	-0.27942	3.850832	-1	-1
34.60798	-22.032	41.02585	-0.91715	-1.27436
-41.5956	-109.906	117.5137	0.361374	-0.42819
-317.946	-435.521	539.2296	0.623087	-0.22136

-190.861	563.6379	595.0762	-0.32625	-0.56866
738.7738	107.0915	746.4954	0.999998	1.917173
482.8411	136.3703	501.7294	0.99832	3.142532
-86.0996	409.6362	418.5869	-0.20714	2.555919
-961.146	1247.213	1574.593	-0.6473	1.602485
-1011.6	-1384.66	1714.822	0.623421	1.165625
1926.308	-230.87	1940.094	-1	-2.83757
-794.547	-260.756	836.2402	0.995498	-2.93735
454.5446	-746.174	873.7198	-0.54354	-5.27951
1062.596	-2165.86	2412.484	-0.4547	-4.10724
-2437.56	2336.056	3376.22	-0.77925	-1.61765
1192.517	369.1771	1248.354	0.996877	3.758072
-922.987	391.1836	1002.461	-0.98231	4.740797
-279.399	1114.906	1149.382	-0.24549	6.462803
3026.018	3185.7	4393.799	0.739727	5.79244
-4301.11	-3423.21	5497.081	0.850083	1.981102
-2361.13	-524.031	2418.588	0.999756	-2.68828
2301.214	-528.117	2361.037	-0.99967	-8.51466
-641.205	-1515.51	1645.57	0.399536	-8.28047
-721.894	-4304.97	4365.079	0.166134	-6.28416
-6314.57	4646.851	7840.092	-0.87614	-2.29618
-6010.86	692.9622	6050.675	-1	3.618096
374.7405	667.5459	765.5377	0.508994	9.817472
1176.563	1942.986	2271.452	0.540982	11.1921
-5632.58	5517.021	7884.381	-0.77025	7.075033
-8105.17	-6011.97	10091.46	0.873621	2.579093
-5123.21	-877.958	5197.891	0.999983	-4.55139

Theodorsen lift Deficiency Factor			
AR	2.3		
K=f			
C ₁	0.248918	C ₂	0.5166522
F	G	C(k)	C _{1c}
0.766741	-0.03965	0.7677659	-4.060903
0.766528	-0.03904	0.7675214	-4.613995
0.766325	-0.03844	0.7672882	-2.002608
0.76613	-0.03786	0.7670656	-1.058584
0.765945	-0.0373	0.7668529	-2.595718
0.765768	-0.03676	0.7666496	4.5327389
0.765599	-0.03623	0.7664551	-0.004524
0.765436	-0.03571	0.7662689	2.6623981

Lift Calculation	
dr	1
c	dL _c
0	0
1	-0.00476
2	-0.03388
3	-0.56559
4	-2.252
5	7.735547
6	-0.00418
7	2.000085

0.765281	-0.03521	0.7660906	4.8130093	8	58.47219
0.765132	-0.03472	0.7659198	4.4245592	9	71.72272
0.76499	-0.03424	0.765756	-1.440903	10	-33.219
0.764853	-0.03378	0.7655988	-0.976074	11	-4.59879
0.764722	-0.03333	0.7654479	4.0581604	12	22.76989
0.764596	-0.03289	0.765303	3.9562263	13	183.3409
0.764475	-0.03246	0.7651638	-4.804322	14	-469.6
0.764358	-0.03205	0.76503	-2.780262	15	-39.8069
0.764247	-0.03164	0.7649012	-4.806011	16	-47.3311
0.764139	-0.03124	0.7647773	0.8588168	17	11.81366
0.764035	-0.03086	0.764658	-2.265186	18	-482.129
0.763935	-0.03048	0.7645431	4.4068217	19	1549.707
0.763839	-0.03011	0.7644323	-2.104329	20	-150.79
0.763746	-0.02975	0.7643256	-3.793399	21	-271.994
0.763657	-0.0294	0.7642226	-4.373396	22	-159.581
0.763571	-0.02906	0.7641232	-0.004689	23	-1.25852
0.763487	-0.02872	0.7640273	-3.593424	24	-3246.89
0.763407	-0.02839	0.7639347	-2.202498	25	-1234.72
0.763329	-0.02807	0.7638452	-1.837359	26	-17.1477
0.763254	-0.02776	0.7637587	-4.708362	27	-401.742
0.763182	-0.02745	0.7636751	3.4161055	28	3641.922
0.763111	-0.02715	0.7635942	2.5597088	29	4630.23
0.763044	-0.02686	0.763516	4.7371757	30	2351.805

Drag Calculation				
		Re ref.	10 ⁵	
		dr	1	
		e	0.8	
		K	4.4	
		C _f	0.006999	
		C _{Dp}	0.030794	
C	C _{di}	dD _i	dD _p	dD _{drag}
0	2.851693	0	0	0
1	3.68139	0.003795	3.17E-05	0.003827
2	0.693505	0.011732	0.000521	0.012253
3	0.19378	0.103534	0.016453	0.119987
4	1.165125	1.010843	0.026716	1.037559
5	3.552867	6.063303	0.052553	6.115856
6	3.54E-06	3.27E-06	0.028488	0.028491
7	1.225755	0.920829	0.023134	0.943962
8	4.005815	48.66577	0.37411	49.03988

9	3.385303	54.87623	0.499175	55.37541
10	0.359027	8.277109	0.709934	8.987043
11	0.164749	0.776219	0.145086	0.921305
12	2.847842	15.97893	0.172782	16.15171
13	2.706573	125.429	1.427067	126.8561
14	3.991368	390.1372	3.009967	393.1472
15	1.336684	19.13822	0.440899	19.57912
16	3.994174	39.33584	0.303269	39.63911
17	0.127544	1.754457	0.423594	2.178051
18	0.887289	188.8531	6.554283	195.4074
19	3.358215	1180.953	10.82904	1191.782
20	0.765746	54.87123	2.206611	57.07784
21	2.488367	178.4207	2.207989	180.6287
22	3.307463	120.6858	1.123641	121.8095
23	3.8E-06	0.00102	8.265787	8.266808
24	2.232927	2017.596	27.82439	2045.42
25	0.838858	470.2647	17.26314	487.5278
26	0.583775	5.448261	0.287395	5.735656
27	3.833515	327.0953	2.627503	329.7228
28	2.017995	2151.391	32.82959	2184.221
29	1.133023	2049.513	55.70294	2105.216
30	3.880579	1926.541	15.2879	1941.829

Normal Force			Vertical Force	
	U(m/s)	4		dF _{ver}
	p	0.000163		-0.10877
				-0.28958
				0.151537
$\ddot{\theta}(t)$	$\ddot{\beta}(t)$	dN _{nc}		-0.72475
0	10667.12	1.136517		-1.49895
-175.051	8848.184	0.932953		4.141026
-399.723	3397.842	0.32617		0.305786
-441.407	-3762.05	-0.45881		1.72753
-130.77	-9901.67	-1.1071		45.18228
510.3484	-12518.9	-1.33956		55.23078
1230.109	-10351.2	-1.03176		-17.3814
1633.535	-3956.46	-0.27596		-2.72668
1370.082	4394.675	0.643298		18.81993
339.9771	11516.63	1.355364		157.6248
-1185.85	14518.83	1.552161		-319.959
-2611.03	11970.82	1.120023		-20.5829
-3233.42	4555.698	0.198804		-24.8922

-2563.47	-5078.28	-0.8607	10.95422
-604.653	-13254.7	-1.62938	-341.264
2045.539	-16666.8	-1.77275	980.9589
4353.584	-13706.9	-1.19479	-78.4467
5238.189	-5195.18	-0.09148	-141.518
4048.572	5813.245	1.113273	-141.183
929.6338	15116.04	1.929581	-2.03951
-3108.59	18962.9	1.999761	-1994.46
-6493.61	15559.23	1.253083	-640.341
-7686.62	5874.509	-0.04923	-14.0393
-5852.26	-6599.95	-1.40326	-330.541
-1319.62	-17100.9	-2.25636	2510.864
4394.291	-21407	-2.2316	2853.084
9067	-17527.5	-1.29194	1219.874
10617.48	-6593.31	0.226561	Lift 122.1587
8001.328	7438.777	1.732906	Lift(N) 1.2215
1779.151	19209.6	2.610129	
-5922.07	23999.25	2.466685	

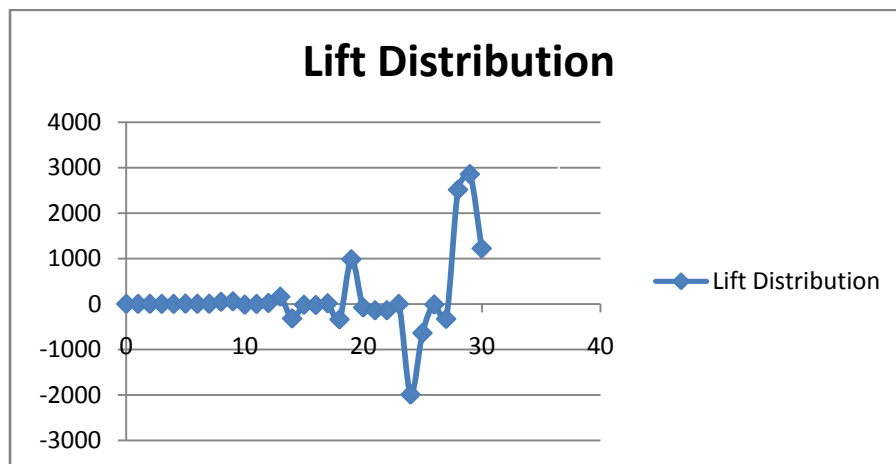


Fig. A.1 Lift distribution curve for flapping wing along span of 40cm

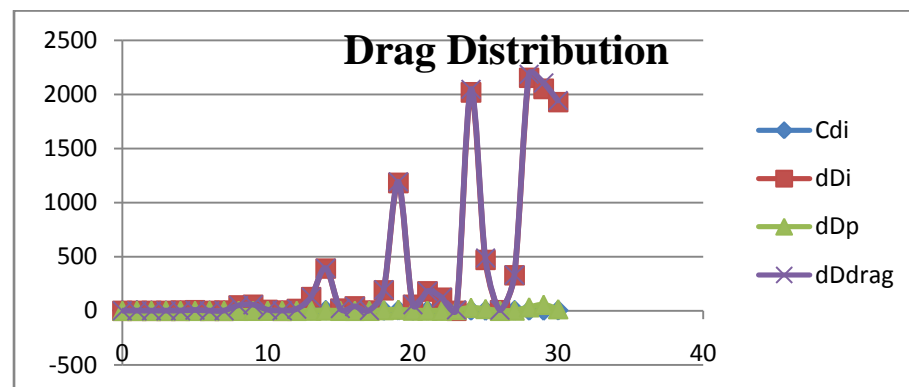


Fig.A.2 Drag distribution curve for flapping wing along span of 40cm.

CONCLUSION:

The goal of this thesis was to develop a MAV capable of hovering flight. The focus was also in the improvement in wing design and controllability. These goals were fully reached. The chosen mechanism for turning rotation of the DC-motors into a flapping movement of the wings is accurate and leads to error free functioning. Through more than 300 tests the wings were optimized in angle and chord length that yield to enough lift generation for hover flight. In order to achieve more lift generation the search space for finding the optimal wing and mechanical configuration can be extended by a smoother discretization and including also the wing shape. There were no improvements on the motors so far. Many suppliers have the same size of DC-Motors but with different parameters, such as velocity constant. Also there should be a betterment in the controllability by calibrating the motors and reducing play in the structure. The gained knowledge can be used for further improvements and opens the way toward an autonomous flapping wing MAV. In addition more improvements can be done in the MAV such as adding a torsional spring and improving the mechanical structure. In addition there can also be the installation of a microcontroller to increase its function capability.

REFERENCES

- [1] Alexander, R. M., *The U J and L of bird flight*, Nature(London), 1997.
- [2] DeLaurier, J. D., *An Aerodynamics Model for Flapping Wing Flight*. The Aeronautical Journal of the Royal Aeronautical Society April 1993, pp.125-130.
- [3] Mueller, T.J., Kellog, J.C., Ifju, P.G., Shkarayev, S.V., *Introduction to the Design of Fixed- Wing Micro Air Vehicles*, AIAA Education Series, AIAA, Reston, Virginia, 2007.
- [4] Liu, C., *Foundations of MEMS*, Pearson Prentice Hall, Upper Saddle River, New Jersey, 2006.
- [5] Freethy, Ron., *How birds work: a guide to bird biology*. Blandford Press. 1982.
- [6] Simkiss, K., *Bird Flight*. Hutchinson Educational Ltd., London. 1963.
- [7] Pennycuick. C. J., *Predicting Wingbeat frequency and wavelength of birds*, 1989, *J.exp biol.*150,171-175.
- [8] Hui hu, AnandGopakumar, Greg Abate, Roberto Albertani, *An experimental investigation on the aerodynamics of flexible membrane in flapping flight*, 2009, *Aerospace Science and Technology* 14(2010) 575-586.
- [9] McMasters, J. H. and Henderson, M. L. 1980. *Low Speed Single Element Airfoil Synthesis*. *Tec. Soaring*;2:1-21.
- [10] Tay. W. B., *Dynamics and Control of a Flapping Wing Aircraft*, M.E. Thesis, National University of Singapore, 2003.
- [11] Shyy, W., Lian, Y., Tang, J., Vieru, D., Liu, H., *“Aerodynamics of Low Reynolds Number Flyers.”*, Cambridge University Press, New York, NY, 2008.
- [12] Norberg, U.M., *“Vertebrate Flight”*, Springer-Verlag, Berlin, 1990, pp. 166-179.
- [13] Whitney. J. P and Wood. R. D., *Conceptual design of flapping wing micro air vehicle*, 2011.
- [14] Muller, T. J., *Fixed and Flapping Wing Aerodynamics for Micro Air Vehicle Applications*. Reston, VA: AIAA, 2001.